Earthline Journal of Chemical Sciences
E-ISSN: 2581-9003; CODEN: EJCSB4
Volume 11, Number 2, 2024, Pages 231-248
https://doi.org/10.34198/ejcs.11224.231248

Some strong dimers of TNAZ - DFT treatment

Lemi Türker

Department of Chemistry, Middle East Technical University, Üniversiteler, Eskişehir Yolu No: 1, 06800 Çankaya/Ankara, Turkey; e-mail: lturker@gmail.com; lturker@metu.edu.tr

Abstract

TNAZ is an explosive material. Presently, some strong dimers of TNAZ have been investigated within the constraints of density functional theory at the level of B3LYP/6-31G(d,p). Core structure of the dimers of consideration is theoretically derived from pseudocyclacene structure by means of certain centric perturbations, and then nitro groups are attached at the desired positions or from two TNAZ molecules via certain intermolecular perturbations. All the present dimers are electronically stable, thermodynamically exothermic and have favorable Gibbs' free energy of formation values at the standard states. Various structural and quantum chemical properties, including UV-VIS spectra have been obtained and discussed.

1. Introduction

TNAZ is a highly nitrated four membered nitrogen heterocyclic ring with greater performance when compared to melt castable explosive, TNT (trinitrotoluene). It has been considered as a potential replacement for TNT because of its low melting point (101 °C) and good thermal stability (up to 240 °C). It was first synthesized by Archibald et al., in 1990 [1]. Several synthesis routes are known [2-4].

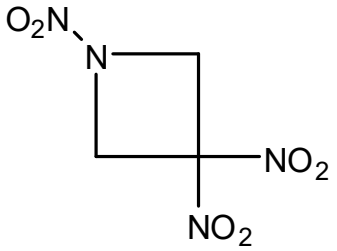

Received: February 24, 2024; Accepted: March 22, 2024; Published: March 25, 2024

Keywords and phrases: TNAZ; 1,3,3-trinitroazetidine; explosive; strong dimers; density functional.

1,3,3-Trinitroazetidine (TNAZ) is a melt-castable explosive [5] having both the N-NO_2 and C-NO_2 groups. The presence of small strained ring system in the structure of TNAZ contributes additional energy [1,3,6,7]. It is also reported that TNAZ is highly energetic material more powerful than RDX, and it is less vulnerable than most other nitramines [2]. Further, TNAZ has many added advantages over known explosives [3]. Unlike HMX, TNAZ is soluble in molten TNT. It possesses improved performance in comparison to conventional melt castable explosive trinitrotoluene (TNT) and is compatible with aluminum, steel, brass and glass. TNAZ provides up to 10% increased energy relative to RDX in the low vulnerability ammunition (LOVA) XM-39 gun propellant formulation [5-9].

An energetic small-ring compound, TNAZ, is the most widely studied explosive in the recent decades [8,9]. For instance, the mobile combustion diagnostic fixture and its application to the study of propellant combustion was reported by Doali et al., [10]. The thermo chemistry of TNAZ was investigated by Wilcox, et al., [11]. Compatibility study of TNAZ with some energetic components was reported by Jizhen et al., [12]. TNAZ based compositions were also investigated [13]. In recent years, TNAZ have been the subject of many theoretical articles [13-19]. By means of molecular dynamics simulation with the ReaxFF/lg reactive force field, Wu et al., investigated the reactive molecular dynamics simulations of the thermal decomposition mechanism of 1,3,3-trinitroazetidine where the thermal decomposition of TNAZ crystals at high temperature was calculated [16]. Thus, authors of the reference managed to analyzed not all of the change in the potential energy of TNAZ, but also the formation of small-molecule products and clusters, and the initial reaction path of TNAZ. Hence, the kinetic parameters of different reaction stages in thermal decomposition of TNAZ were obtained [16].

In the present density functional treatise, some strong dimers of TNAZ molecule have been the focus of investigation in terms of various aspects.

2. Method of Calculations

In the present study, all the initial optimizations of the structures leading to energy minima have been achieved first by using MM2 method which is then followed by semi empirical PM3 self consistent fields molecular orbital method [20-22]. Afterwards, the structure optimizations have been achieved within the framework of Hartree-Fock and finally by using density functional theory (DFT) at the level of B3LYP/6-31G(d,p) [23,24]. Note that the exchange term of B3LYP consists of hybrid Hartree-Fock and local

spin density (LSD) exchange functions with Becke's gradient correlation to LSD exchange [25]. Note that the correlation term of B3LYP consists of the Vosko, Wilk, Nusair (VWN3) local correlation functional [26] and Lee, Yang, Parr (LYP) correlation correction functional [27]. In the present study, the normal mode analysis for each structure yielded no imaginary frequencies for the 3*N*–6 vibrational degrees of freedom, where *N* is the number of atoms in the system considered. This search has indicated that the structure of each molecule corresponds to at least a local minimum on the potential energy surface. Furthermore, all the bond lengths have been thoroughly searched in order to find out whether any bond cleavage occurred or not during the geometry optimization process. All these computations were performed by using SPARTAN 06 [28].

3. Results and Discussion

The cage structure of strong dimers of TNAZ can be considered as derived from pseudocyclacene molecule [29-32] which could be obtained via certain intra molecular perturbations [33,34] whereas the pseudocyclacene molecule theoretically is obtained by means of intermolecular union of two 4-membered rings. The pseudocyclacene structure has certain peculiarities for theoretical considerations. It has two 4-membered rings standing for the top and bottom peripheral circuits if the whole structure is assumed to be a cyclacene molecule. It has R = 2 but in reality there exists a single nonplanar benzenoid ring [29].

Figure 1 shows a weak dimer of TNAZ in which a singly bound carbon-carbon bond exists between rings.

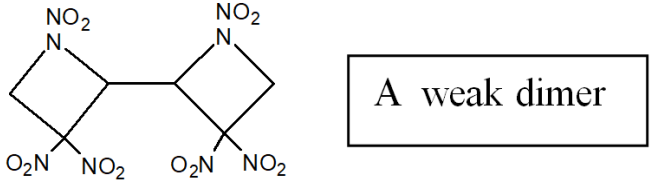

Figure 1. A weak dimer of TNAZ.

Figure 2 shows some types of strong dimers of TNAZ in which one or two doubly bounded carbon-carbon bond(s) exists between the upper and lower rings (decks). However, structures of strong dimers should exhibit some peculiarities due to the structure of the parent hydrocarbon cage (pseudocyclacene) from which they have been derived [29-32].

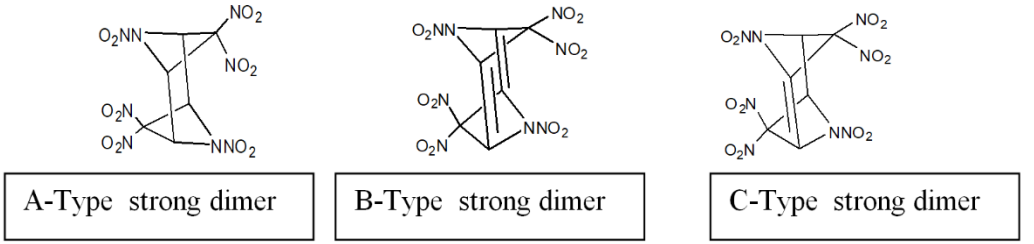

Figure 2. Some types of strong dimers of TNAZ.

Although the upper and lower decks have butterfly stereo form, they might undergo some interaction. In the case of B- and C-type of dimers, the presence of longitudinal double bond(s) may be in conjugation with the nitramine group(s), in spite of the fact that a partial conjugation may exist as long as the hybridization of the carbon atoms allows. However, the double bond(s) may have π-π type interactions. All these facts make these structures interesting and mater of investigation theoretically, although they are not existing yet (up to the best knowledge of the author).

Figure 3 displays the optimized structures of various strong types of TNAZ dimers.

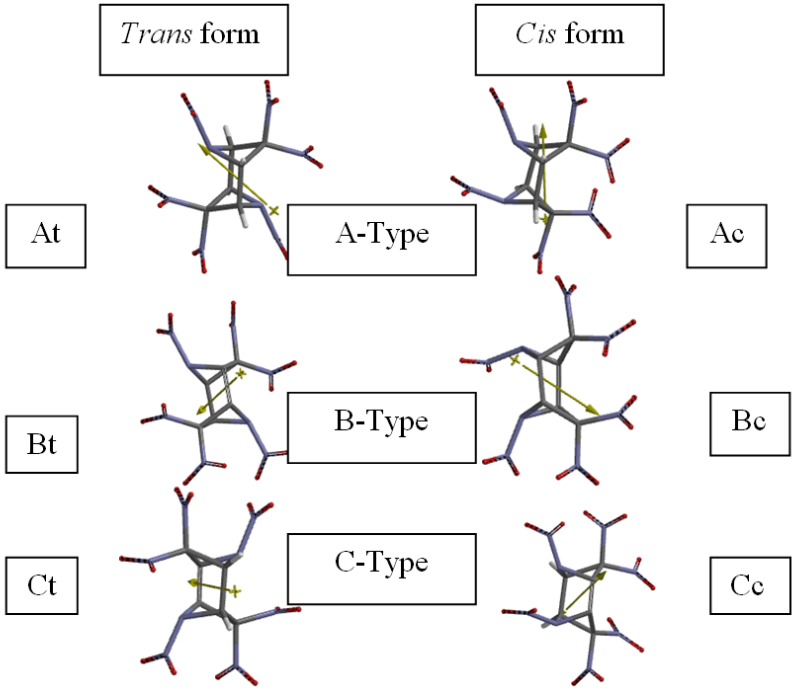

Figure 3. Optimized structures of various strong types of TNAZ dimers.

The figure also shows the direction of the dipole moment vectors. The labels in Figure 3 stand for the types of the strong dimers shown in Figure 2 as well as their *cis* or *trans* forms, such as At, Ac, etc. The capital letters (A,B,C) indicate the class of the compound as defined above whereas lowercase letters (c or t) stand for the stereoisomers, namely cis or trans forms.

Figure 4 shows the chiral centers of the dimers considered. Note that dimers of B-series do not have any chiral centers at all.

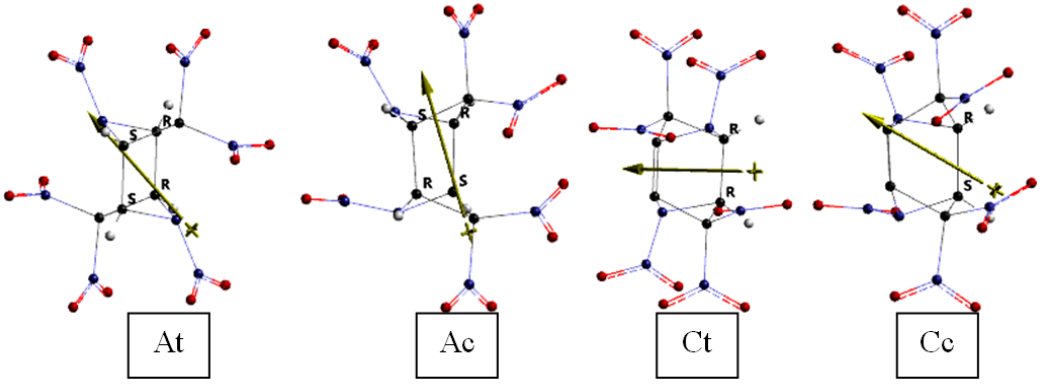

Figure 4. Chiral centers of the dimers considered.

Also note that the geometrical isomerism of the strong dimers presently considered is defined with respect to the plane passing through the longitudinal bonds connecting the upper and lower decks. Also note that in the *cis* form of the dimers the nitramine nitro groups of the upper and lower decks have been inclined in to the same direction.

Figure 5 shows the calculated bond lengths of the strong types of TNAZ dimers considered. As seen in the figure in all the cases the longitudinal double bonds connecting the decks are longer than the carbon-carbon double bonds, for instance in B-series they are in between 1.50-1.65 Å. Whereas in C-series they are about 1.36 Å. There should be some repulsive forces, either electronic or/and steric, operating between the decks.

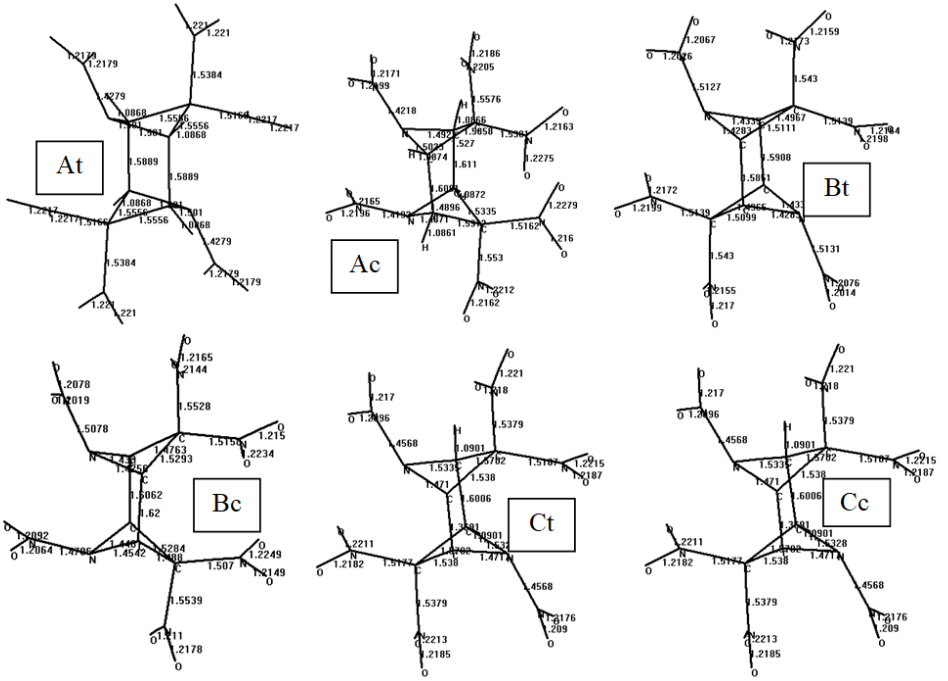

Figure 5. Bond lengths of the strong types of TNAZ dimers considered.

In Table 1, one finds some thermo chemical values of the dimers considered. All the structures considered are exothermic and the algebraic order of H^o values is At < Ac <Ct < Cc < Bt < Bc. The results indicate that in all the dimer series (the series are not structurally isomeric) the *trans* isomer is more exothermic than the respective *cis* isomer. All the isomers have favorable Gibbs' free energy of formations at the standard states. Also in all the series, the *trans* stereoisomer possesses more favorable G^o value compared to the corresponding *cis* isomer.

Table 1. Some thermo chemical values of the dimers considered.

Dimers	H^o	S^o (J/mol^o)	G^o
At	-4124003.796	552.49	-4124168.548
Ac	-4123941.938	551.86	-4124106.48
Bt	-4117182.863	557.83	-4117349.19
Bc	-4117118.144	557.67	-4117284.418
Ct	-4120536.237	552.94	-4120701.094
Cc	-4120468.761	552.28	-4120633.434

Energies in kJ/mol.

Table 2 lists some energies of the dimers considered where E, ZPE and E_C stand for the total electronic energy, zero point vibrational energy and the corrected total electronic energy, respectively. As the data reveal, all of the structures are electronically stable. The algebraic order of E_C values is At < Ac <Ct < Cc < Bt < Bc.

Table 2. Some energies of the dimers considered.

Dimers	E	ZPE	E_C
At	-4124458.85	445.01	-4124013.84
Ac	-4124397.94	445.95	-4123951.99
Bt	-4117502.76	309.55	-4117193.21
Bc	-4117436.59	307.72	-4117128.87
Ct	-4120923.33	377.12	-4120546.21
Cc	-4120856.32	377.51	-4120478.81

Energies in kJ/mol.

Table 3 includes some structural properties of the dimers considered.

Table 3. Some geometrical properties of the dimers considered.

Dimers	Area (Å²)	Volume (Å³)	PSA (Å²)	Ovality
At	294.60	253.38	241.954	1.52
Ac	283.87	252.82	231.404	1.47
Bt	289.54	247.83	243.706	1.52
Bc	281.39	247.38	235.482	1.48
Ct	289.60	250.18	241.053	1.51
Cc	281.23	249.64	232.173	1.47

It is worth mentioning that the polar surface area (PSA) is defined as the amount of molecular surface area arising from polar atoms (N,O) together with their attached hydrogen atoms.

Some other properties of the dimers considered are collected in Table 4. As seen in the table in each case of series, the *trans* form has more negative aqueous energy (Eaq

values) than the *cis* form. This order is opposite to the dipole moment values, namely *cis* form possesses greater dipole moment. On the other hand, the polarizability is defined according to the multivariable formula [28].

$$\text{Polarizability} = 0.08*V - 13.0353*h + 0.979920*h^2 + 41.3791$$

where V and h are the Van der Waals volume and hardness, respectively. Hardness is defined as,

$$\text{Hardness} = -(\varepsilon_{HOMO} - \varepsilon_{LUMO})/2$$

where ε_{HOMO} and ε_{LUMO} are the molecular orbital energies of the highest occupied (HOMO) and the lowest unoccupied (LUMO) molecular orbital energies, respectively.

Note that all the dimers considered have positive log P values. It is worth mentioning that a negative value for log P means the compound has a higher affinity for the aqueous phase (it is more hydrophilic); when log P = 0 the compound is equally partitioned between the lipid and aqueous phases; a positive value for log P denotes a higher concentration in the lipid phase (i.e., the compound is more lipophilic).

Table 4. Some properties of the dimers considered.

Dimers	Eaq (kJ/mol)	Dipole (debye)	Polarizability	Log P
At	-4124455.27	0.03	60.76	2.87
Ac	-4124389.69	1.07	60.68	2.87
Bt	-4117442.18	0.08	60.35	0.69
Bc	-4117371.72	0.21	60.44	0.69
Ct	-4120903.18	1.94	60.65	1.78
Cc	-4120833.35	2.43	60.66	1.78

Point group of all is C1. Polarizabilities in 10^{-30} m^3 units.

Figure 6 displays the electrostatic potential (ESP) maps of the dimers considered where negative potential regions coincide with red/reddish and positive ones with blue/bluish parts of the maps. As seen in the figure, almost all the present dimers possess an intense positive potential region over the cage atoms. The isomers of B-series have lower intensity in the respective region. It is to be noted that the ESP charges are obtained by the program based on a numerical method that generates charges that reproduce the electrostatic potential field from the entire wavefunction [28].

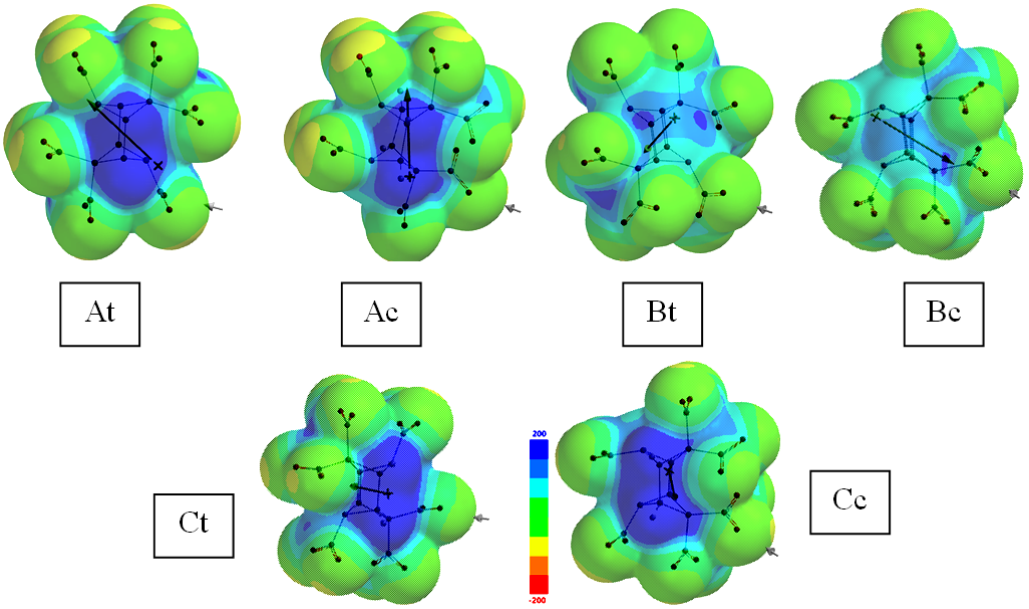

Figure 6. The ESP maps of the dimers considered.

Table 5 lists the HOMO and LUMO (frontier molecular orbitals) energies and the interfrontier molecular orbital energy gap ($\Delta\varepsilon=\varepsilon_{LUMO}-\varepsilon_{HOMO}$) values of the molecules considered.

Table 5. The HOMO, LUMO energies and Δε values of the dimers considered.

Dimers	HOMO	LUMO	Δε
At	-867.02	-390.85	476.17
Ac	-879.72	-390.36	489.36
Bt	-854.70	-394.20	460.5
Bc	-828.62	-418.59	410.03
Ct	-883.00	-468.77	414.23
Cc	-858.33	-464.40	393.93

Energies in kJ/mol.

Figure 7 displays some of the molecular orbital energy levels of the dimers considered. As seen in the figure and Table 5, in A- series the *cis* form has lower HOMO energy compared to the *trans* isomer. Whereas in the cases of B- and C- series the trans isomer possesses the lower HOMO energy. As for the LUMO energies, in A- and C-series the *trans* isomer has the lower LUMO energy compared to the respective value of the *cis* isomer. Consequently, $\Delta\varepsilon$ values of the *trans* isomer in the cases of B- and C-series are greater than the respective value of the *cis* isomer which is opposite to the case of A-series. Note that the energy spacing between the HOMO and NEXTHOMO or LUMO and NETLUMO are highly characteristic feature of the structure of the dimer as well as the *cis* and *trans* forms considered. The overall order of $\Delta\varepsilon$ values is Cc < Bc < Ct < At < Bt < Ac.

Note that the impact sensitivity of explosives are related to the interfrontier molecular orbital energy gap values. That is narrower the gap, the explosive becomes more sensitive to an impact stimulus [34,35]. Thus, dimer-Cc and dimer-Ac should be the most and the least sensitive to impact stimulus, respectively. This outcome should have arisen from the electronic perturbations resulting from orientation of the nitro groups present as well as the peculiarities of the rings in the dimers. The strong dimers considered possess embedded TNAZ moiety in their structures and additionally some of which contain longitudinal carbon-carbon double bonds. Hence, they should have some similar properties with TNAZ. However, as a conjecture, the presence of extra rings should make them to have some acute explosive properties compared to TNAZ.

Figure 8 shows the calculated (time-dependent DFT) UV-VIS spectra of the dimers considered. The data from the figure indicate that in the cases of A and B-series of dimers with the exception of dimer-Bc, absorb only in the ultraviolet region of the spectrum. In the others a shoulder emerges and its skirts intrude into the visible part of the spectrum (bathochromic shift) while the λ_{max} of Bc shifts to lower part as well (some sort of hypsochromic shift). The λ_{max} values of At and Ac are 312.43 nm and 299.83nm; whereas for Bt and Bc they are 320.52 nm and 314.65, 345.39 nm, respectively. As for the C-series, λ_{max} values are 309.47 nm, 321.69 nm for Ct and 347.56 nm for Cc. A comparison of λ_{max} values reveals that their order does not strictly follow the expected opposite order of $\Delta\varepsilon$ values (see Table 5). Because the spectra are dictated not only by the transitions involving the HOMO-LUMO energy gap but some other orbital energy gaps are effective as well. The differences of intensities over the comparable regions suggest that the transition moments responsible for the peaks considered should be quite different.

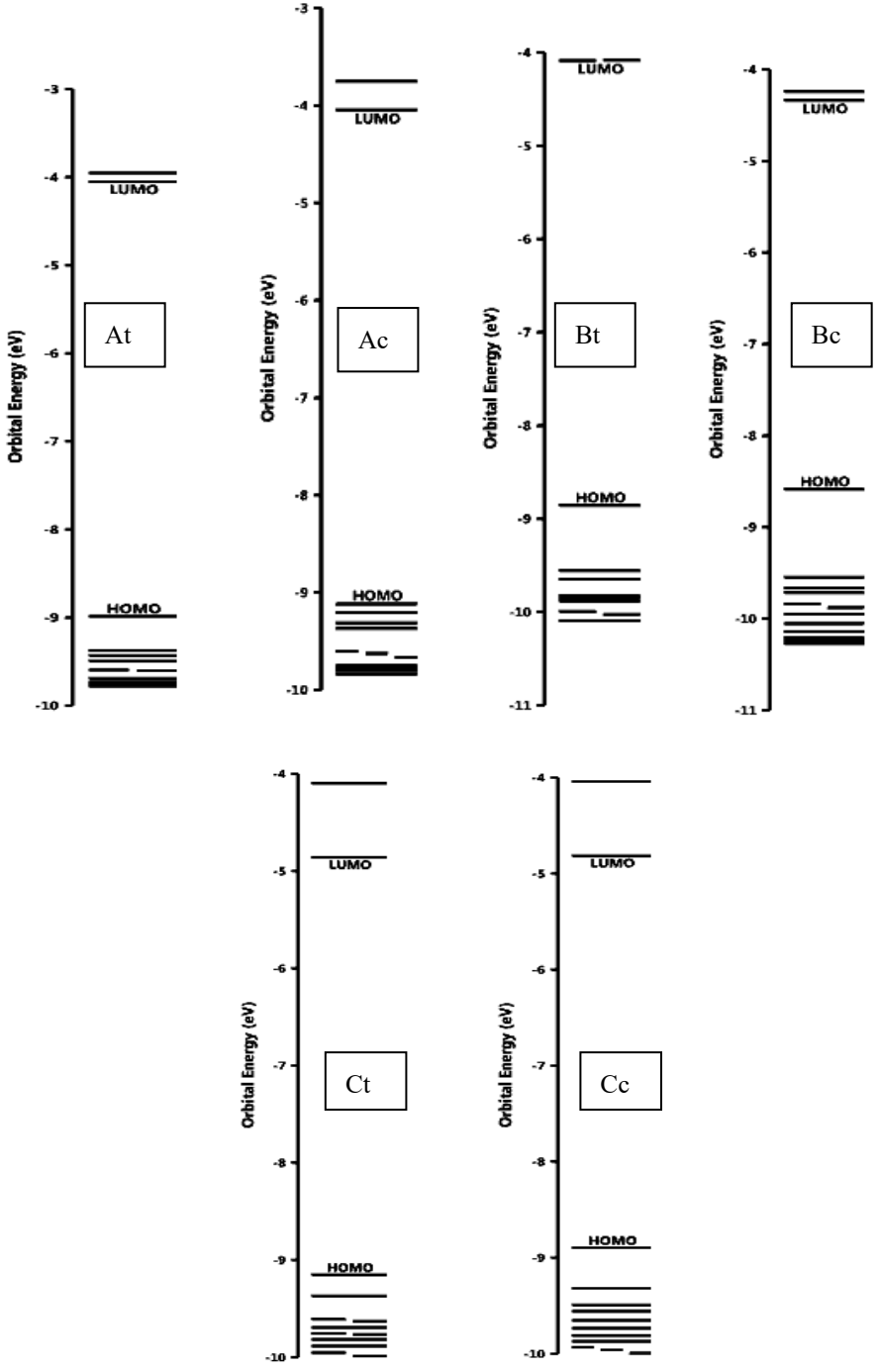

Figure 7. Some of the molecular orbital energy levels of the dimers considered.

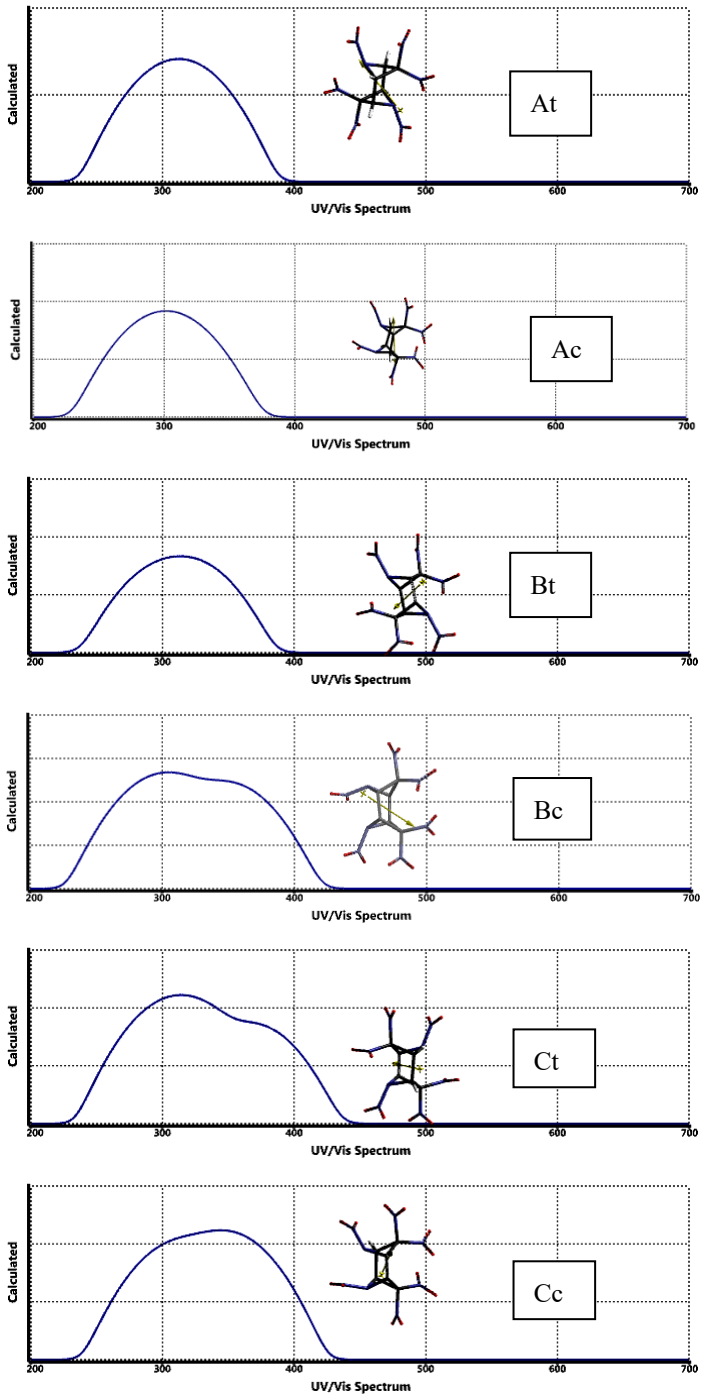

Figure 8. The calculated UV-VIS spectra of the dimers considered.

Figure 9 shows the local ionization maps of the molecules considered where conventionally red/reddish regions (if any exists) on the density surface indicate areas from which electron removal is relatively easy, meaning that they are subject to electrophilic attack. As seen in the figure, core region of At, Ac, and C-type dimers are dark blue in contrast to the respective regions of Bt, Bc and (especially) Cc-types.

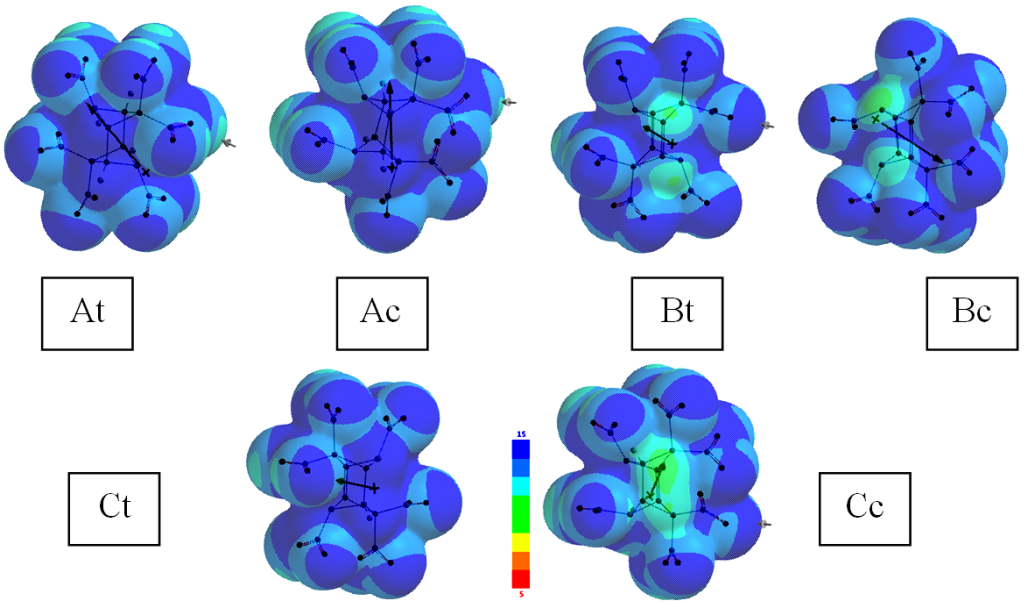

Figure 9. The local ionization maps of the dimers considered.

Figure 10 shows the LUMO maps of the dimers considered. Note that a LUMO map displays the absolute value of the LUMO on the electron density surface. The blue color (if any exists) stands for the maximum value of the LUMO and the red colored region, associates with the minimum value. As seen in the figure, the core regions of A-series of dimers associates with dark red color in contrast to the respective region of the others.

Note that the LUMO and NEXTLUMO are the major orbitals directing the molecule towards the attack of nucleophiles. Positions where the greatest LUMO coefficient exists is the most vulnerable site in nucleophilic reactions.

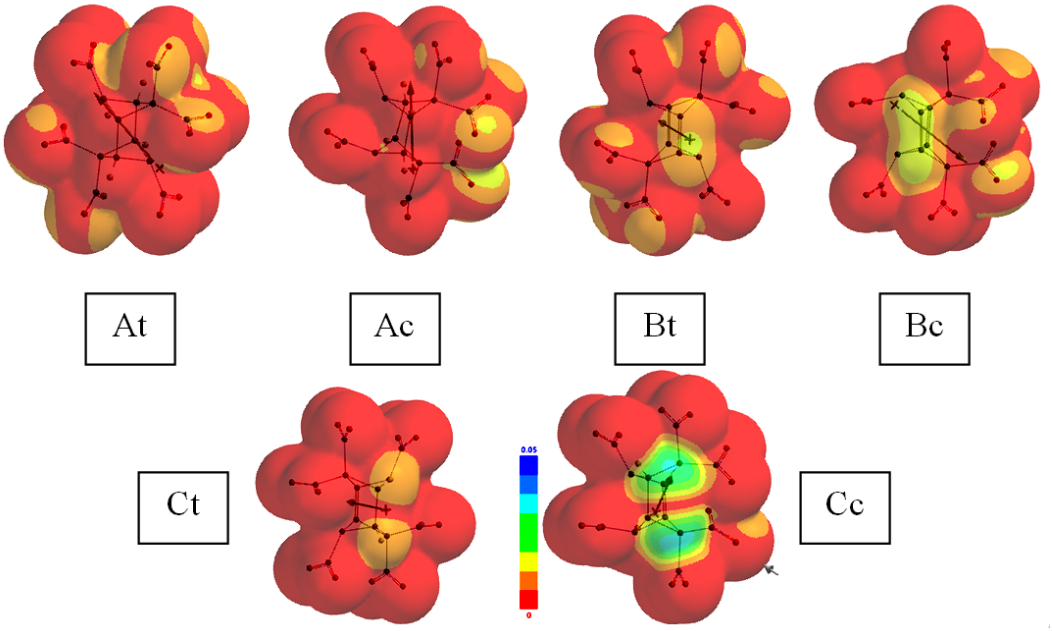

Figure 10. The LUMO maps of the dimers considered.

4. Conclusion

The present study on the strong dimers of TNAZ, within the restrictions of density functional theory and the level of basis set employed has revealed that all the dimers considered are thermodynamically exothermic, electronically stable and have favorable Gibbs' free energy of formations at the standard states. In all the cases, the *trans* isomer is more exothermic and electronically more stable than the respective *cis* isomer. The reason could be not only the steric factors but also the electronic effects especially in the case of B-type dimers due to the partial conjugative effects involving the nitramine group and the longitudinal double bonds. Both types of steric and electronic effects should have dictated some other properties including the ballistic properties of these nonexistent dimers.

References

[1] Archibald, T.G., Gilardi, R., Baum, K., & George, C. (1990). Synthesis and x-ray crystal structure of 1,3,3-trinitroazetidine. *The Journal of Organic Chemistry*, *55*(9), 2920-2924. https://doi.org/10.1021/jo00296a066

[2] Viswanath, D.S., Ghosh, T.K., & Boddu, V.M. (2018). 1,3,3-Trinitroazetidine (TNAZ). In T. M. Klapötke & J. Stierstorfer (Eds.), *Emerging energetic materials: Synthesis, physicochemical, and detonation properties* (pp. 293-307). Dordrecht, Netherlands: Springer. https://doi.org/10.1007/978-94-024-1201-7_11

[3] Zdenek, J., Zeman, S., Suceska, M., Vávra, P., Dudek, K., & Rajic, M. (2001). 1,3,3-trinitroazetidine (TNAZ). Part I. Syntheses and properties. *Journal of Energetic Materials*, *19*(2), 219-239. https://doi.org/10.1080/07370650108216127

[4] Axenrod, T., Watnick, C., Yazdekhasti, H., & Dave, P. R. (1993). Synthesis of 1,3,3-trinitroazetidine. *Tetrahedron Letters, 34*(42), 6677-6680. https://doi.org/10.1016/S0040-4039(00)61673-8

[5] Ducan, S.W., & Mathew, D.C. (2000). Evaluation of 1,3,3-trinitroazetidine (TNAZ) – A high performance melt-castable explosive, DSTO Aeronautical and Maritime Research Laboratory, P.O. Box 4331, Melborne-Victoria 3001, Australia AR-011-500, July 2000 and ibid, TNAZ based melt-cast explosives: Technology review and ARML Research Directions, DSTO-TR-0702, Aeronautical and Maritime Research Laboratory (AMRL)-DSTO, Fishermans Bed, 1998.

[6] McKenney, R.L., Jr., Floyd, T.G., Stevens, W.E., Archibald, T.G., Marchand, A.P., Sharma, G.V.M., & Bott, S.G. (1998). Synthesis and thermal properties of 1,3-dinitro-3-(1′,3′-dinitroazetidin-3′-yl) azetidine (TNDAZ) and its admixtures with 1,3,3-trinitroazetidine (TNAZ). *J. Energ. Mater*., *16*, 199-235. https://doi.org/10.1080/07370659808217513

[7] Hiskey, A.M., Johnson, M.C., & Chavez, E.D. (1999). Preparation of 1-substituted-3,3-dinitroazetidines. *J. Energ. Mater.*, *17*, 233-252. https://doi.org/10.1080/07370659908216106

[8] Pagoria, P.F., Lee, G.S., Mitchell, R.A., & Schmidt, R.D. (2002). A review of energetic materials synthesis. *Thermochim. Acta., 384*, 187-204. https://doi.org/10.1016/S0040-6031(01)00805-X

[9] Jadhav, H.S., Talawar, M.B., Dhavale, D.D., Asthana, S.N., & Krishnamurthy, V.V. (2006). Alternate method to synthesis of 1,3,3-trinitroazetedine (TNAZ): Next generation melt castable high energy material. *Indian J. Chem. Technol., 13*, 41-46. http://nopr.niscair.res.in/handle/123456789/8455

[10] Doali, J.O., Fifer, R.A., Kruzezynski, D.I., & Nelson, B.J. (1989). The mobile combustion diagnostic fixture and its application to the study of propellant combustion Part-I. Investigation of the low pressure combustion of LOVA XM-39 Propellant, Technical report No. BRLMR-3787/5, US Ballistic Research Laboratory, Maryland, 1989.

[11] Wilcox, C.F., Zhang, Y.-X., & Bauer, S.H. (2000). The thermo chemistry of TNAZ (1,3,3-trinitroazetidine) and related species: models for calculating heats of formation. *Journal of Molecular Structure: THEOCHEM.*, *528*(1-3), 95-109. https://doi.org/10.1016/S0166-1280(99)00475-3

[12] Jizhen, L., Xuezhong, F., Xiping, F., Fengqi, Z., & Rongzu, H. (2006). Compatibility study of 1,3,3-trinitroazetidine with some energetic components and inert materials. *Journal of Thermal Analysis and Calorimetry*, *85*(3), 779-784. https://doi.org/10.1007/s10973-005-7370-8

[13] Iyer, S., Sarah, Y., Yoyee, M., Perz, R., Alster, J., & Stoc, D. (1992). III, TNAZ based composition C-4 development, 11th Annual Working Group, Institute on Synthesis of High Density Materials (Proc.), Kiamesha Lakes, 1992.

[14] Oftadeh, M., Hamadanian, M., Radhoosh, M., & Keshavarz, M.H. (2011). DFT molecular orbital calculations of initial step in decomposition pathways of TNAZ and some of its derivatives with –F, –CN and –OCH3 groups. *Computational and Theoretical Chemistry, 964*, 262-268. https://doi.org/10.1016/j.comptc.2011.01.007

[15] Türker, L., & Varis, S. (2012). Desensitization of TNAZ via molecular structure modification and explosive properties – A DFT study. *Acta Chim. Slov*., *59*, 749-759.

[16] Wu, J., Huang, Y., Yang, L., Geng, D., Wang, F., Wang, H., & Chen, L. (2018). Reactive molecular dynamics simulations of the thermal decomposition mechanism of 1,3,3-trinitroazetidine. *Chem. Phys. Chem*., *19*(20), 2683-2695. https://doi.org/10.1002/cphc.201800550

[17] Türker, L. (2021). Some ions of TNAZ - A DFT Study. *Earthline Journal of Chemical Sciences*, *6*(2), 215-228. https://doi.org/10.34198/ejcs.6221.215228

[18] Türker, L. (2020). A DFT treatment of some aluminized 1,3,3-trinitroazetidine (TNAZ) systems - A deeper look. *Earthline Journal of Chemical Sciences*, *3*(2), 121-140. https://doi.org/10.34198/ejcs.3220.121140

[19] Türker, L. (2021). Effect of selenium on TNAZ molecule - A DFT treatment. *Earthline Journal of Chemical Sciences*, *6*(1), 119-135. https://doi.org/10.34198/ejcs.6121.119135

[20] Stewart, J.J.P. (1989). Optimization of parameters for semi-empirical methods I. *J. Comput. Chem.*, *10*, 209-220. https://doi.org/10.1002/jcc.540100208

[21] Stewart, J.J.P. (1989). Optimization of parameters for semi-empirical methods II. *J. Comput. Chem., 10*, 221-264. https://doi.org/10.1002/jcc.540100209

[22] Leach, A.R. (1997). *Molecular modeling*. Essex: Longman.

[23] Kohn, W., & Sham, L.J. (1965). Self-consistent equations including exchange and correlation effects. *Phys. Rev., 140*, 1133-1138. https://doi.org/10.1103/PhysRev.140.A1133

[24] Parr, R.G., & Yang, W. (1989). *Density functional theory of atoms and molecules*. London: Oxford University Press.

[25] Becke, A.D. (1988). Density-functional exchange-energy approximation with correct asymptotic behavior. *Phys. Rev. A*, *38*, 3098-3100. https://doi.org/10.1103/PhysRevA.38.3098

[26] Vosko, S.H., Wilk, L., & Nusair, M. (1980). Accurate spin-dependent electron liquid correlation energies for local spin density calculations: a critical analysis. *Can. J. Phys*., *58*, 1200-1211. https://doi.org/10.1139/p80-159

[27] Lee, C., Yang, W., & Parr, R.G. (1988). Development of the Colle-Salvetti correlation energy formula into a functional of the electron density. *Phys. Rev. B*, *37*, 785-789. https://doi.org/10.1103/PhysRevB.37.785

[28] SPARTAN 06 (2006). Wavefunction Inc. Irvine CA, USA.

[29] Türker, L. (2003). An *ab initio* treatment on some isomeric structures of a small pseudocyclacene. *Journal of Molecular Structure (THEOCHEM).*, *637* (1-3), 109-113. https://doi.org/10.1016/S0166-1280(03)00473-1

[30] Türker, L. (1999). PM3 treatment of monoazacyclacenes. *Journal of Molecular Structure: THEOCHEM., 492*(1-3), 159-163. https://doi.org/10.1016/S0166-1280(99)00157-8

[31] Türker, L. (1994). Cryptoannulenic behavior of cyclacenes. *Polycyclic Aromatic Compounds, 4*(3), 191-197. https://doi.org/10.1080/10406639408014703

[32] Türker, L., & Gümüş, S. (2004). Cyclacenes. *Journal of Molecular Structure: THEOCHEM.*, *685*(1-3) , 1-33. https://doi.org/10.1016/j.theochem.2004.04.021

[33] Dewar, J.M.S. (1969). *The molecular orbital theory of organic chemistry*. New York: McGraw-Hill.

[34] Dewar, M.J.S., & Dougherty, R.C. (1975). *The PMO theory of organic chemistry*. New York: Plenum/Rosseta.

[35] Anbu, V., Vijayalakshmi, K.A., Karunathan, R., Stephen, A.D., & Nidhin, P.V. (2019). Explosives properties of high energetic trinitrophenyl nitramide molecules: A DFT and AIM analysis. *Arabian Journal of Chemistry*, *12*(5), 621-632. https://doi.org/10.1016/j.arabjc.2016.09.023

[36] Badders, N.R., Wei, C., Aldeeb, A.A., Rogers, W.J., & Mannan, M.S. (2006). Predicting the impact sensitivities of polynitro compounds using quantum chemical descriptors, *Journal of Energetic Materials*, *24*, 17-33. https://doi.org/10.1080/07370650500374326